THE JOURNAL OF PHYSICAL CHEMISTRY C

Article

pubs.acs.org/JPCC

Quantitative Characterization of Hexagonal Packings in Nanoporous Alumina Arrays: A Case Study

José R. Borba,[†,§] Carolina Brito,[†,§] Pedro Migowski,[‡] Tiberio B. Vale,[†,∥] Daniel A. Stariolo,[†] Sérgio R. Teixeira,[†] and Adriano F. Feil*[,†,⊥]

[†]Instituto de Física, Universidade Federal do Rio Grande do Sul − IF-UFRGS, P.O.Box 15051, 91501-970, Porto Alegre-RS, Brasil

[‡]Instituto de Química, Universidade Federal do Rio Grande do Sul − IQ-UFRGS, P.O.Box 15003, 91501-970, Porto Alegre-RS, Brasil

Supporting Information

ABSTRACT: Herein is presented a methodology to quantify the degree of hexagonal order in nanoporous alumina arrays (NAA). The approach is inspired by the theory of two-dimensional melting, developed to describe phase transitions in two-dimensional systems that present liquid-crystal-like structures. A local order parameter (LOP) is defined to quantify the degree of hexagonal order of each pore without any arbitrary parameters. Using this LOP, three main qualitative and quantitative analytical tools were developed: (i) a color code to create a map of the LOP, which is a visual tool to identify the degree of order; (ii) quantitative measurements of the average hexagonal order of the sample by measuring the distribution of the LOP and the distribution of the number of neighbors of each pore, and (iii) a quantification of the spatial correlation of the LOP, which indicates how far the hexagonal order is spread in a sample. Because this approach has a strong support on tools developed in statistical mechanics, one can go beyond a simple characterization and interpret the results in terms of phases, as in other physical systems. This may help to unveil the mechanisms behind the self-organization process and long-range order observed in NAA. Moreover, this approach can be trivially extended to characterize other physical systems that form hexagonal packings.

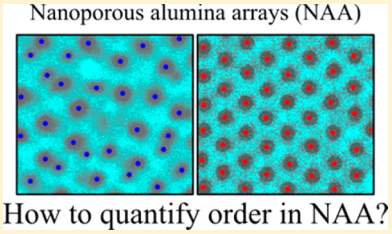

INTRODUCTION

Since Keller,[1] the nanoporous alumina arrays (NAA) formed by aluminum anodization can be considered to be the most popular self-organized hexagonal packing system. The high interest in this methodology is mainly due to its simplicity and low cost. For many engineering applications, such as high-density magnetic recording media,[2] photonic crystals,[3] or pattern-transfer masks,[4] the ordering and organization of the NAA is a crucial factor. When a high degree of regularity and uniformity is required for applications, it is very important to quantify the level of ordering in a NAA structure.

The anodization process is normally realized in two anodization steps and under time-consuming potentiostatic conditions to obtain a high ordering degree.[5] The auto-organization of the nanopores is a phenomenon controlled by anodization parameters, as the applied voltage, temperature, type, and concentration of electrolyte[6−11] and characteristics of the aluminum matrix.[12−14] It is already known that the control of these parameters can lead to structures with a low or high degree of structural organization. The usual method to characterize the degree of ordering is qualitative, normally visual or using Fourier analysis.[15−19] These approaches are limited, revealing patterns that just allow a qualitative identification of the lattice type, but the relation with the underlying long-range ordering of the NAA lattice is not revealed. To date, few methodologies for the quantitative characterization of hexagonal packing systems were developed.

Different methods have been proposed to characterize quantitatively the degree of ordering of the NAA, mainly based on calculation of Radial Distribution Function (RDF).[20,21] Pichler et al.[22] proposed a method based on autocorrelation functions that could be applied to a wide range of superstructures, but the order parameters proposed rely on purely empirical fitting procedures of autocorrelations. Hillebrand et al.[23] used Delaunay triangulation to define a network of pores in contact and compare it with a perfect hexagonal network. They also propose an algorithm to define a grain of nearly ideal pores through the introduction of a "quality threshold." This method is very useful, allowing the determination of grains and measures of the grain size, although it relies on a somewhat arbitrary threshold parameter.[24]

It is important to have a tool to characterize the degree of order of the self-assembled structures, which is simple to implement and of wide applicability to different structures. Moreover, it should give meaningful information that can be compared and predicted from model systems. From this point of view, it is important to get in contact with observables from statistical mechanics. Systems that can form crystal-like superstructures, like NAA or colloidal nanocrystals, may develop two different kinds of order. The positional order represents the translational invariance of the center of mass of the unit cells structures, for example, pore centers, and orientational order associated with rotational invariance of

Received: August 28, 2012
Revised: December 4, 2012
Published: December 4, 2012

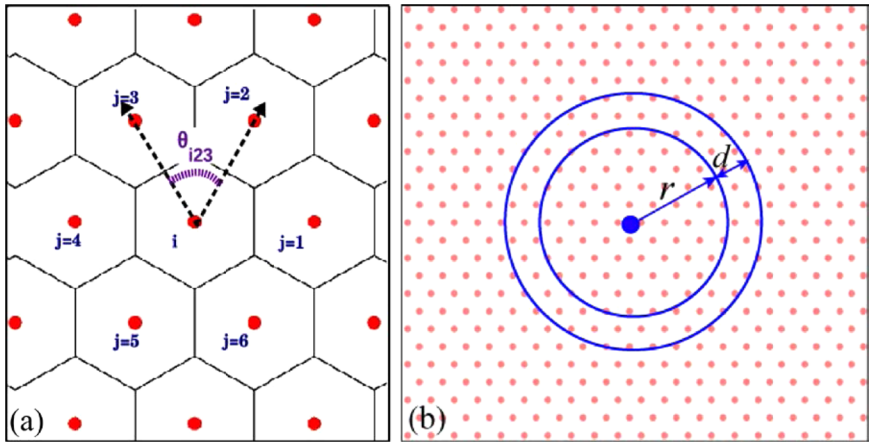

Figure 1. (a) Example of a determination of nearest neighbors for a hexagonal lattice. In this case, the Voronoi cells are hexagons, and the neighbors of a given point i are the j points that are in the neighbor cells. The angle θ_{i23} is defined between the lines that connects the sites i to 2 and i to 3. (b) Sketch of the computation of the spatial correlation $C_6^i(r)$. Circles represent the centers of the points distributed in a hexagonal lattice and the (red) color represents the value of ψ_6 of each point. The $C_6^i(r)$ is a measure of the correlation between the particle i and all n_{ring} particles inside of the colored ring.

bonds or edges connecting vertices of the crystal lattice and the orientation of the sides of triangles or hexagons, as in self-assembled NAA. Both kinds of order can be characterized through suitable order parameters and associated correlation functions. For two-dimensional structures, a comprehensible description of the onset of order is given by the theory of 2D melting, or KTHNY theory, after the names Kosterlitz–Thouless–Halperin–Nelson–Young, who pioneered in the statistical description of phase transitions mediated by topological defects. A review of this theory can be seen in refs 25 and 26. A crystalline structure without any defects shows both positional and orientational order. Positional order can be conveniently quantified by means of RDF, which presents distinct peaks at the positions of the density maxima when the system is in a crystal phase. As soon as the structure presents topological defects (e.g., dislocations), the positional order is disrupted, and the RDF decays exponentially. Nevertheless, these defects do not destroy the orientational order completely. An intermediate phase, called the "hexatic phase," with short-range positional order and quasi-long-range orientational order, is possible. In the hexatic phase, positional correlations decay exponentially, but orientational correlations decay much more slowly, as a power law of the distance from any fixed point in the lattice. A suitable orientational order parameter is the so-called "hexatic parameter," which will be defined below and used to characterize the orientational order of NAA.

Correlations of the hexatic order parameter can quantify the extension of hexagonal order in the lattice. At still higher degrees of disordering, other kinds of topological defects, that is, isolated disclinations, can appear. These are isolated particles with five or seven nearest neighbors. When isolated disclinations proliferate, orientational correlations decay exponentially, and the system loses both translational and orientational order, as in a fluid phase.

In this article, we propose the use of statistical mechanical tools to describe experimental systems that form hexagonal networks, like NAA. The local order parameter (LOP) was quantified by defining an order parameter for hexagonal packing, which is a natural quantity in the theory of 2D melting. Suitably defined correlations of the hexatic order parameter allowed further quantification of the degree of order in the lattice. Other quantities of interest, like the distribution of the number of neighbors, could also be easily measured and related to the order parameter. Using statistical mechanical quantities to characterize order is useful because (i) there are no arbitrary parameters, (ii) the proposed implementation is quite simple, and (iii) it allows making contact with results from model systems, which can further open new perspectives on the relevance and influence of the control of the anodization parameters in experiments.

METHODOLOGY

Methodology for Quantitative Characterization of Hexagonal Packing System. In this section, we describe a general method to characterize the degree of order of hypothetical points distributed in a sample. In the following sections, we will apply the method to NAA. Details of the quantification method to characterize the hexagonal packing system can be seen in a web site developed to facilitate the readers analyzing their hexagonal systems.[27]

Let us first suppose that one has the coordinates of N points distributed in a sample in two dimensions. The methodology to quantify the orientational order of this sample can be summarized in the following steps:

Determination of Nearest Neighbors. To define the nearest neighbors of a point i, one can use a distance criterion, in which all points that are below a given distance d_{th} from point i are considered to be its neighbors. However, here we avoid the arbitrariness in the parameter d_{th} by constructing the Voronoi diagram of the sample.[28] This procedure associates, for each point i, a corresponding Voronoi cell, namely, the set of all points whose distance to i is smaller than their distance to the other points. This allows us to define unambiguously the n_n^i nearest neighbors of each point i. In Figure 1a, there is an example of the Voronoi diagram for a hexagonal lattice.

Computation of a Local Order Parameter, ψ_6^i. For each point i, we compute

$$\psi_6^i = \frac{1}{n_n^i}\sum_{j=1}^{n_n^i}\cos(6\theta_{ijk}) \quad (1)$$

dx.doi.org/10.1021/jp308542d | J. Phys. Chem. C 2013, 117, 246–251

where n_n^i is the number of nearest neighbors of point i and θ_{ijk} is the angle between the lines that connect the sites i to j and i to k, as exemplified in Figure 1a by the point i and its neighbors j = 2 and k = 3. Note that $\psi_6^i = 1$ if point i and its neighbors describe a perfect hexagon.

Computation of the Spatial Correlation of the LOP, C_6. Once ψ_6^i is computed for all points in the sample, this defines a field of the LOP. We then define the spatial correlation of this field as:

$$C_6^i(r) = \langle \psi_6^i \psi_6^j \rangle_r = \frac{1}{n_{\text{ring}}(r)} \sum_{j=1}^{n_{\text{ring}}(r)} \psi_6^i \psi_6^j \tag{2}$$

where the $\langle \psi_6^i \psi_6^j \rangle_r$ indicates an average over all $n_{\text{ring}}(r)$ points that are at a distance between r and $r + dr$ from point i (blue ring in Figure 1b), and then this value is averaged over the whole sample:

$$C_6(r) = \frac{1}{N} \sum_{i=1}^{N} C_6^i(r) \tag{3}$$

To exemplify the method and which type of measures one can extract from it, consider two extreme cases: (i) a hexagonal lattice of points and (ii) a completely random network of points. The results are summarized in Figure 2a,b, respectively.

The Voronoi diagram and the color-coded map of ψ_6, Figure 2a,b, show visually a clear difference between the cases. One observes that the Voronoi cells are irregular and the values of ψ_6 are not homogeneous in the random distribution case, Figure 2b, in clear contrast with what happens in the hexagonal lattice, Figure 2a. The inhomogeneity of the values of ψ_6 is an important measure to characterize the degree of hexagonal order in a sample. The distribution of ψ_6, $\rho(\psi_6)$ quantifies the degree of (in)homogeneity. For the hexagonal case, the distribution will be peaked at $\psi_6 = 1$, whereas the random case displays a Gaussian distribution with an average given by $\langle \psi_6 \rangle = 0$, as shown in Figure 2c.

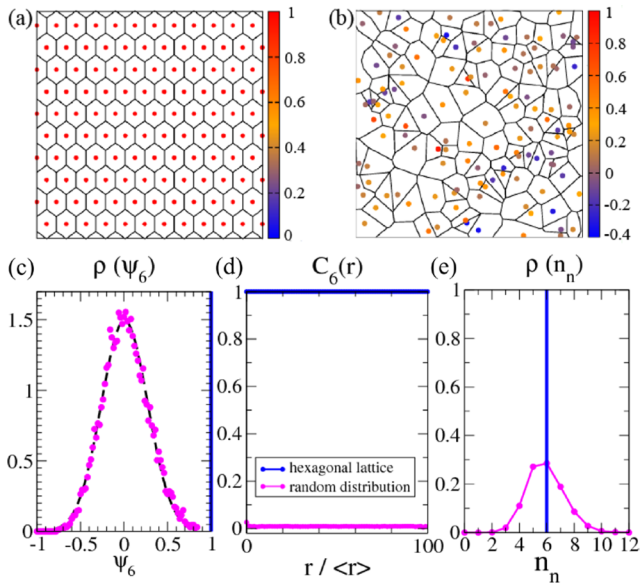

Figure 2. Voronoi diagram and the map of ψ_6 for all points (a) in the hexagonal lattice and (b) in a completely random case. The color code on the right of each Figure corresponds to the value of ψ_6. (c) The distribution of LOP, $\rho(\psi_6)$. The slashed line represents the Gaussian distribution fitted to the randomly spaced points. The blue vertical line at $\psi_6 = 1$ marks the distribution of the hexagonal lattice. (d) The spatial correlation of ψ_6, $C_6(r)$. The x axis is normalized by the mean distance between the points in a sample. (e) The distribution of the number of neighbors, which has a peak in $n_n = 6$ for the hexagonal packing (blue line) and a Gaussian distribution around 6 in the case of the random distribution of points.

One can go beyond this local analysis of the order and compute the spatial correlation of ψ_6. The quantity $C_6(r)$ informs us how far the LOP ψ_6 is correlated in space. The correlation functions for the two examples considered are shown in Figure 2d. If the sample describes a perfect hexagonal lattice, with $\psi_6^i = 1$ for all i, then it does not matter how far two points i and j are, the correlation between ψ_6^i and ψ_6^j will be 1. In the other extreme, if points are distributed randomly, then even two nearest neighbors are uncorrelated, and C_6 decays to zero very quickly. It is important to notice that the most valuable information that can be extracted from C_6 is the way it decays; that is, its functional dependence. When C_6 decays exponentially, this decay is related to the typical sizes of the regions where ψ_6 has the same value. This is related to the typical grain size of a sample. At large separations, the asymptotic value of C_6 is $\langle \psi_6 \rangle^2$.

A third important quantity to evaluate the hexagonal order in a sample is the distribution of neighbors, shown in Figure 2e. For a perfect hexagonal lattice, each point has exactly six neighbors, whereas in any other case, the number of neighbors is distributed around this value; the deviation from this value increases with the disorder. As described, in a hexagonally ordered array, points with five or seven neighbors are related to topological defects of the lattice. Depending on the neighborhood, they can form dislocations or disclinations, and their presence characterizes hexatic or disordered structures, with specific forms for the decay of orientational correlations.

As we described in the Introduction, there are two kinds of order to completely characterize hexagonal phase in a real solid,[25] the positional order and the orientational order. However, in our samples, we found that orientational correlations decay at best as a power law of the distance from a particular site. In this case, it is expected that positional correlations, which are more sensitive to defects, decay faster, typically exponentially fast. We have indeed verified this, computing the RDF for our samples. This quantity, then, would not help to quantify different levels of order in the samples, and for this reason, we did not include an analysis of RDF in our work.

Formation of NAA by Al Anodization. For the quantitative characterization of hexagonal packing arrays, three different samples of NAA structure were prepared by anodization process. The process was carried out in two anodization steps, in a conventional two-electrode cell using a Cu sheet as a cathode.[12−14,29−33] The anode is made of Al with two different degrees of purity, that is, high-purity Al Bulk (99.999%) and commercial Al (99.5%). After each anodization step, the samples were dipped in a 5 wt % H_3PO_4 solution at 35 ± 1 °C for different times to remove the alumina formed in the first anodization step. A second anodization step was performed to allow the opening of nanopores. Table 1 summarizes the anodization conditions, and the name that will be used for each sample.

After the anodization process, the morphological nanoporous structure was characterized by scanning electron microscopy

dx.doi.org/10.1021/jp308542d | J. Phys. Chem. C 2013, 117, 246−251

Table 1. Anodization Conditions Used for the Three Different Alumina Nanoporous Samples

		anodization steps			
		1st		2nd	
sample name	material	condition	etching (min)	condition	etching (min)
S1	Al (99.999%)	[a]	50	[a]	10
S2	Al (99.999%)	[b]	90	[b]	30
S3	Al (99.5%)	[a]	30	[a]	10

[a] 0.3 M H_2SO_4, 25 V at 3 ± 2 °C for 12 h. [b] 0.3 M $H_2C_2O_4$, 30 V at 15 ± 2 °C for 12 h.

(SEM, JEOL JSM 6060) operating at 20 kV acceleration voltages.

SEM Micrographs Graphical Treatments for the Application of Statistical Mechanical Models. The next step was to characterize how close to the hexagonal lattice the samples were. Before applying the statistical mechanical models described in the previous section, it was necessary to obtain the coordinates of the nanopores center. To do so, we adjusted ellipses for each nanopore, totalling 1245 nanopores for S1, 484 for S2, and 977 nanopores for S3. This allows the definition of the center of mass of each nanopore, and the values of the major and minor semi axes of the ellipses are related to the size of the pores. This was done with a standard software package, for example, ImageJ.[34] Thus, it was possible to obtain for each sample the average nanopore diameter (d) from the average of the major and minor semi axes and the interpore distance (h) from the center of mass of each nanopore. Details of this procedure can be seen in the Supporting Information.

RESULTS AND DISCUSSION

Figure 3a–c shows the SEM images of the S1, S2, and S3 samples, respectively, prepared with different Al characteristics and anodization parameters, as described in the previous section (Table 1). The anodization of the S1, S2, and S3 yielded NAA with d of 22.0 ± 0.4, 61.9 ± 1.2, and 39.2 ± 1.3 nm and h of 54.4 ± 0.4, 90.6 ± 1.2 and 74.6 ± 1.5 nm, respectively. The images treatment procedure for the characterization of the nanopore dimensions can be seen in detail in the Supporting Information, Figure SI2, and the results are summarized in Table SI1 in the Supporting Information. The obtained anodization results indicate that distinct structures were formed, leading to different visual levels in the nanopores order. The S1 and S2 samples show a higher ordering level of NAA compared with S3. This result is due to the higher purity of the Al matrix in the S1 and S2 samples, whereas the S3 sample presents more impurities, which hampers the formation of NAA with hexagonal order. The Voronoi diagram and the map of ψ_6 were used as a systematic procedure to quantify the degree of order of the different anodization systems, as shown in Figure 3d–f. A visual inspection on the S1 sample indicates many more red points (corresponding to $\psi_6 = 1$ in the color code) and that they are concentrated in regions where the Voronoi cells are hexagonal. Moreover, it is possible to observe that the hexagonal order is decreasing from the S1 to the S3 samples, and for the last ones, there are very few red points.

Figure 4a–c summarizes the quantitative analysis of nanopore ordering with the distribution of the LOP ψ_6, correlations C_6, and the number of neighbors $\rho(n_n)$, respectively. For sample S1, $\rho(\psi_6)$ has a mean value $\langle\psi_6\rangle \approx 0.79$, and the distribution is completely asymmetric, indicating that most of the nanopores form hexagons with their neighbors. Sample S2 is also asymmetric and has most of the nanopores with a large value of $\langle\psi_6\rangle = 0.56$, but the standard deviation ($\sigma = 0.34$) from the average value indicates more disorder than in sample S1. The S3 sample shows approximately a symmetric distribution around $\langle\psi_6\rangle = 0.27$. This indicates that the sample is much more disordered than the previous cases (S1 and S2 samples), but it still has ~30% more order than the completely random case, for which $\langle\psi_6\rangle = 0$. The dashed Gaussian curve drawings in Figure 4a–c represent the distribution for a random set of points discussed in the Methodology Section and are a benchmark of such a completely disordered case.

The middle column of Figure 4a–c, C_6 indicates how far ψ_6 is correlated in space. The x axis is normalized by the mean distance between the nanopores. It is important to note that in sample S1, the correlation decays very slowly, after 20 nanopores (which corresponds to more than half of the system size in this case), and the correlation is ~60% of the nearest

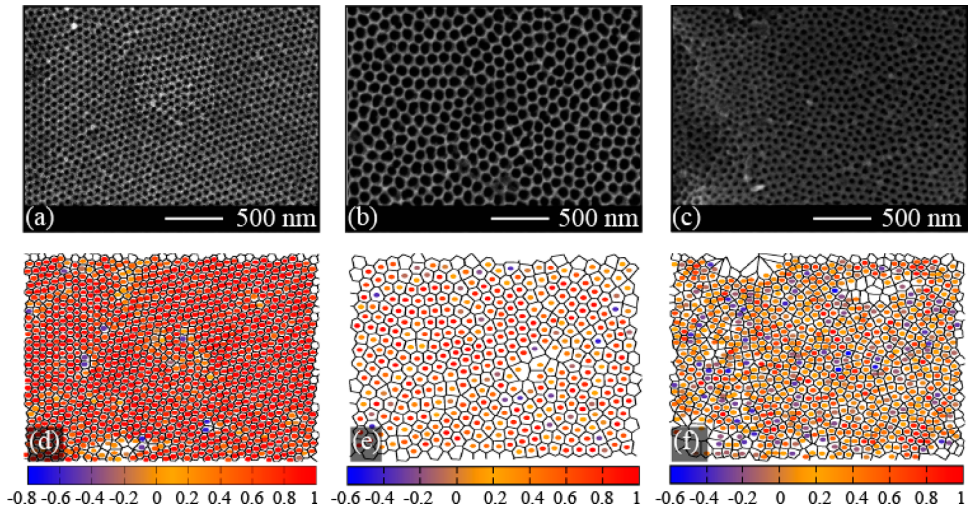

Figure 3. SEM images of the experimental samples of alumina nanopores: (a) S1, (b) S2, and (c) S3. (d–f) Quantitative map of the ψ_6 and the Voronoi diagram for the respective samples. The colors indicate the value of ψ_6 for each nanopore. The color code is below each Figure.

dx.doi.org/10.1021/jp308542d | J. Phys. Chem. C 2013, 117, 246–251

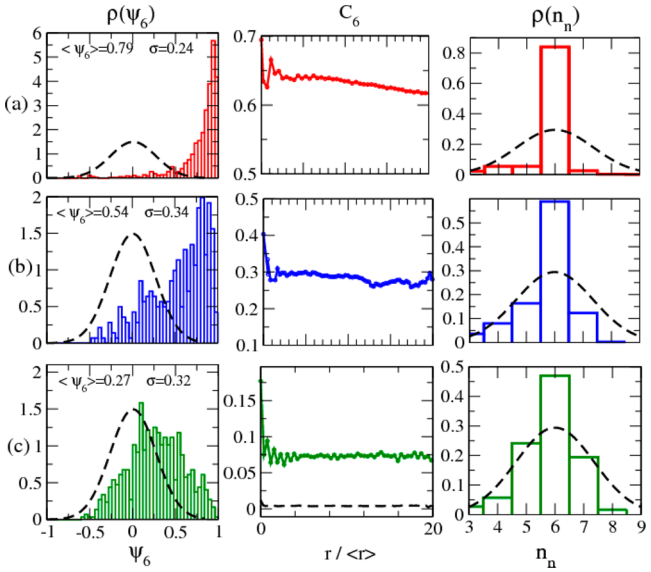

Figure 4. First column: distribution of ψ_6, $\rho(\psi_6)$. Second column: correlation of ψ_6, C_6. Third column: distribution of the number of neighbors, $\rho(n_n)$. In each line, we show all quantities for different samples, from (a) to (c), in the same order as in Figure 3. In all Figures we plot dashed curves that represent the random distribution of points discussed in the Methodology Section and are used here to be compared with the samples of NAA.

neighbor value. For sample S2, although the absolute value of the correlation is smaller than in the S1 case, the decay of C_6 is also slow. C_6 for sample S3 shows that after two nanopores, the values of C_6 are not correlated anymore, suggesting that the grain size is comparable to the size of a pore.[12]

The distribution of neighbors shows that the dispersion around the value $n_n = 6$ increases from S1 to S3, also pointing to an increase in the disorder.

One can rationalize the results obtained for these samples in the light of the theory of 2D melting, or KTHNY theory.[25,26] The most ordered sample analyzed here, S1, is not a perfectly ordered sample. The presence of defects is evident from the distributions $\rho(\psi_6)$ and $\rho(n_n)$. Because the correlations of the order parameter decay slowly, the behavior is analogous to the hexatic phase. Sample S2 also has a behavior of its correlation function analogous to a hexatic phase, although it has more defects than the sample S1. The picture changes for sample S3. In this case, the system still has more defects, and they are enough to destroy completely the correlation of ψ_6. As can be seen in Figure 4c, C_6 decays very fast, typically exponentially with the distance from any point in space. If a fit to an exponential decay, $C_6 \approx e^{(-r/x_i)}$, could be possible, then x_i might be interpreted as a typical grain size of the sample, which is too small in this case, being only about two to three interpore distances. This result can be interpreted as a result of the impurities present in the Al matrix. It is important to emphasize that the robustness of this statistical characterization method was checked in detail, as can be seen in the Supporting Information, Figure SI3.

CONCLUSIONS

In this article, we proposed a systematic methodology to characterize hexagonal arrays of NAA based on statistical tools that have been previously developed to describe melting in 2D systems. For each nanopore, its neighbors were defined using Voronoi tessellation; then, an LOP called the hexatic order parameter was defined, ψ_6, to quantify how close a given nanopore is to a perfect hexagon. The correlation of this parameter at two different points of the array, C_6, informs us how long the local orientational order spreads in the sample.

The method was first presented for a hypothetical network of points and used to compute the defined quantities for two extreme cases, a perfectly hexagonal network and a completely random distribution of points. All realistic physical systems stay in between these two theoretical limits. Then, the developed tools were applied to the NAA. The average value of ψ_6 quantifies the degree of orientational order in a sample, and its standard deviation is a measure of how heterogeneous the local order is in the sample. The correlation of this hexatic order parameter characterizes the range of the local order and allows a determination of the size of highly ordered grains on the sample.

We stress that this method can be easily extrapolated to characterize any kind of system that presents hexagonal networks. As soon as one is able to treat the experimental images and define the center of mass of the pores, the method is quite general and easy to implement and has no arbitrary parameters.

Other works have been proposed to quantify the hexagonal order in NAA. However, the approach presented herein is inspired by a theory developed long ago to describe phase ordering in 2D systems. General key features necessary to display melting in 2D systems can be borrowed from that theory to model the growth of the NAA. We expect that this way of characterizing order in NAA and the analogy to other physical systems showing hexagonal packing arrays will help to improve the theoretical modeling to better understand the development of long-range order in the NAA and similar systems, from which better suited experiments can be devised.

ASSOCIATED CONTENT

Supporting Information

Details of the NAA SEM images treatments and complementary characterization of the NAA hexagonal packing systems. The document also presents the distribution of distance between neighbor pores h, distribution of major semiaxis $\rho(a)$ and minor semiaxis $\rho(b)$, and the distribution of the $d = (a + b)/2$, $\rho(d)$, for the three samples S1, S2, and S3. This material is available free of charge via the Internet at http://pubs.acs.org.

AUTHOR INFORMATION

Corresponding Author

*E-mail: affeil@if.ufrgs.br.

Present Addresses

[‖]Instituto de Ensino Superior do Noroeste Fluminense – INFES, Universidade Federal Fluminense – UFF, Santo Antônio de Pádua-RJ, Brasil.

[⊥]Energy Sciences, National Renewable Energy Laboratory, Golden, CO 80401, USA.

Author Contributions

[§]These authors contributed equally.

Funding

The authors declare no competing financial interests.

Notes

The authors declare no competing financial interests.

■ ACKNOWLEDGMENTS

This work was partially sponsored by CNPq (no. 471220/2010-8), FAPERGS (no. 11/2000-4), and CAPES (Brazilian funding agencies). Thanks also to the "Centro de Microscopia Eletrônica (CME) of the Universidade Federal do Rio Grande do Sul." The authors also thank Mr. Gustavo T. Cabral by the development of the website that characterizes quantitatively the NA.

■ REFERENCES

(1) Keller, F.; Hunter, M. S.; Robinson, D. L. *J. Electrochem. Soc.* **1953**, *100*, 411−419.
(2) Baik, J. M.; Schierhorn, M.; Moskovits, M. *J. Phys. Chem. C* **2008**, *112*, 2252−2255.
(3) Gadot, F.; Chelnokov, A.; DeLustrac, A.; Crozat, P.; Lourtioz, J. M.; Cassagne, D.; Jouanin, C. *Appl. Phys. Lett.* **1997**, *71*, 1780−1782.
(4) Wang, Y. D.; Zang, K. Y.; Chua, S. J.; Sander, M. S.; Tripathy, S.; Fonstad, C. G. *J. Phys. Chem. B* **2006**, *110*, 11081−11087.
(5) Masuda, H.; Fukuda, K. *Science* **1995**, *268*, 1466−1468.
(6) Jessensky, O.; Muller, F.; Gosele, U. *Appl. Phys. Lett.* **1998**, *72*, 1173−1175.
(7) Li, A. P.; Muller, F.; Birner, A.; Nielsch, K.; Gosele, U. *J. Appl. Phys.* **1998**, *84*, 6023−6026.
(8) Li, F. Y.; Zhang, L.; Metzger, R. M. *Chem. Mater.* **1998**, *10*, 2470−2480.
(9) Lee, W.; Ji, R.; Gosele, U.; Nielsch, K. *Nat. Mater.* **2006**, *5*, 741−747.
(10) Chu, S. Z.; Wada, K.; Inoue, S.; Isogai, M.; Yasumori, A. *Adv. Mater.* **2005**, *17*, 2115−2119.
(11) Nielsch, K.; Choi, J.; Schwirn, K.; Wehrspohn, R. B.; Gosele, U. *Nano Lett.* **2002**, *2*, 677−680.
(12) Feil, A. F.; da Costa, M. V.; Amaral, L.; Teixeira, S. R.; Migowski, P.; Dupont, J.; Machado, G.; Peripolli, S. B. *J. Appl. Phys.* **2010**, *107*, 026103.
(13) Feil, A. F.; da Costa, M. V.; Migowski, P.; Dupont, J.; Teixeira, S. R.; Amaral, L. *J. Nanosci. Nanotechnol.* **2011**, *11*, 2330−2335.
(14) Feil, A. F.; Migowski, P.; Dupont, J.; Amaral, L.; Teixeira, S. R. *J. Phys. Chem. C* **2011**, *115*, 7621−7627.
(15) Li, A. P.; Muller, F.; Gosele, U. *Electrochem. Solid State Lett.* **2000**, *3*, 131−134.
(16) Rahimi, M. H.; Saramad, S.; Tabaian, S. H.; Marashi, S. P.; Zolfaghari, A.; Mohammadalinezhad, M. *Appl. Surf. Sci.* **2009**, *256*, 12−16.
(17) Napolskii, K. S.; Roslyakov, I. V.; Eliseev, A. A.; Petukhov, A. V.; Byelov, D. V.; Grigoryeva, N. A.; Bouwman, W. G.; Lukashin, A. V.; Kvashnina, K. O.; Chumakov, A. P.; Grigoriev, S. V. *J. Appl. Crystallogr.* **2010**, *43*, 531−538.
(18) Leitao, D. C.; Apolinario, A.; Sousa, C. T.; Ventura, J.; Sousa, J. B.; Vazquez, M.; Araujo, J. P. *J. Phys. Chem. C* **2011**, *115*, 8567−8572.
(19) Winkler, N.; Leuthold, J.; Lei, Y.; Wilde, G. *J. Mater. Chem.* **2012**, *22*, 16627−16632.
(20) Kaatz, F. H. *Naturwissenschaften* **2006**, *93*, 374−378.
(21) Matefi-Tempfli, S.; Matefi-Tempfli, M.; Piraux, L. *Thin Solid Films* **2008**, *516*, 3735−3740.
(22) Pichler, S.; Bodnarchuk, M. I.; Kovalenko, M. V.; Yarema, M.; Springholz, G.; Talapin, D. V.; Heiss, W. *ACS Nano* **2011**, *5*, 1703−1712.
(23) Hillebrand, R.; Muller, F.; Schwirn, K.; Lee, W.; Steinhart, M. *ACS Nano* **2008**, *2*, 913−920.
(24) Abdollahifard, M. J.; Faez, K.; Pourfard, M.; Abdollahi, M. *Appl. Surf. Sci.* **2011**, *257*, 10443−10450.
(25) Nelson, D. R. *Defects and Geometry in Condensed Matter Physics*; Cambridge University Press: Cambridge, U.K., 2002.
(26) Gasser, U.; Eisenmann, C.; Maret, G.; Keim, P. *ChemPhysChem* **2010**, *11*, 963−970.
(27) http://www.lief.if.ufrgs.br/~cbrito/nanoporos/.
(28) Atsuyuki, O.; Barry, B.; Kokichi, S. *Spatial Tessellations: Concepts and Applications of Voronoi Diagrams*; John Wiley & Sons, Inc.: 1992; p 532.
(29) Feil, A. F.; Migowski, P.; Scheffer, F. R.; Pierozan, M. D.; Corsetti, R. R.; Rodrigues, M.; Pezzi, R. P.; Machado, G.; Amaral, L.; Teixeira, S. R.; Weibel, D. E.; Dupont, J. *J. Braz. Chem. Soc.* **2010**, *21*, 1359−1365.
(30) Weibel, D. E.; Michels, A. F.; Feil, A. F.; Amaral, L.; Teixeira, S. R.; Horowitz, F. *J. Phys. Chem. C* **2010**, *114*, 13219−13225.
(31) Feil, A. F.; Weibel, D. E.; Corsetti, R. R.; Pierozan, M. D.; Michels, A. F.; Horowitz, F.; Amaral, L.; Teixeira, S. R. *ACS Appl. Mater. Interfaces* **2011**, *3*, 3981−3987.
(32) Wender, H.; Feil, A. F.; Diaz, L. B.; Ribeiro, C. S.; Machado, G. J.; Migowski, P.; Weibel, D. E.; Dupont, J.; Teixeira, S. R. *ACS Appl. Mater. Interfaces* **2011**, *3*, 1359−1365.
(33) Goncalves, R. V.; Migowski, P.; Wender, H.; Eberhardt, D.; Weibel, D. E.; Sonaglio, F. C.; Zapata, M. J. M.; Dupont, J.; Feil, A. F.; Teixeira, S. R. *J. Phys. Chem. C* **2012**, *116*, 14022−14030.
(34) ImageJ, public domain. http://rsbweb.nih.gov/ij/.